

Study on 1-allyl-3-butylimidazolium Bromine as Corrosion Inhibitor for X65 Steel in 0.5 M H₂SO₄ Solution

Li Luo¹, Shengtao Zhang^{1,*}, Yujie Qiang^{1,2,**}, Nanxi Chen¹, Shenyang Xu^{1,4}, Shijin Chen³

¹School of Chemistry and Chemical Engineering, Chongqing University, Chongqing 400044, P.R. China

²Sichuan University of Science and Engineering, Zigong, Sichuan 643000, P.R. China

³Bomin electronics Ltd, Meizhou, Guangdong 514021, P.R. China

⁴School of Chemistry and Chemical Engineering, Yibin University, Sichuan 644000, P.R. China

*E-mail: stzhang_cqu@163.com, 20141802032@cqu.edu.cn

Received: 18 July 2016 / Accepted: 20 August 2016 / Published: 6 September 2016

In this paper, the anti-corrosive effect of an ionic liquid named 1-allyl-3-butylimidazolium bromine for X65 steel in 0.5 M H₂SO₄ has been systematically studied via various electrochemical techniques, containing weight loss experiments, electrochemical tests, scanning electron microscope (SEM), theoretical calculations. The results obtained from weight loss experiments and electrochemical tests displayed that [ABIm]Br served as a mixed-type inhibitor primarily controlling cathode corrosion process and the anti-corrosive efficiency (up to 90.38% at 10 mM) improved with the increase of the concentration. Besides, it was found that the adsorption of the organic molecules on X65 steel substrate followed the Langmuir adsorption isotherm and surface topography of X65 steel was characterized using Scanning electron microscopy (SEM). In addition, theoretical calculations suggested that investigated inhibitor was flat-lying adsorbed on the X65 steel surface.

Keywords: X65 steel, Ionic liquids, Weight loss, Electrochemical tests, Theoretical calculations

1. INTRODUCTION

With the development of national economy, pipeline steels have being increased significantly to meet the demands and widely used in various fields, petroleum exploring and exploiting, petroleum refining, gases and liquids transporting, construction and so on[1-4]. But corrosion causes tremendously detrimental impact in industrial processes under natural conditions, especially in acidic medium[5-7], since the acidic solutions are widely applied to the pickling, cleaning, acid de-scaling of metal[5, 8-12].

There are quietly various methods to suppress the disadvantageous process of corrosion, such as protective coatings, electrochemical protection (cathodic protection, anodic protection), alloying, corrosion inhibitor. Inhibitors are the substances which have an obvious effect on controlling, reducing or prohibiting reactions at the metal/solution interface by adding a little to the aggressive medium[13, 14].

The bulk of corrosion inhibitors are organic compounds which have been extensively employing to anti-corrode by means of heteroatoms (O, N, P, S) and multiple bonds generally in the molecular structure[15-20]. These molecules are normally adsorbed on the metal surface to decrease the corrosion rate. The process of adsorption rely upon the distribution of electronic and inhibitor structure[21-23]

Nevertheless, With the development of economy and the aware of protecting-environment, many organic inhibitors have been questioned, for they have a negative influence on environment-friendly society[24-26]. For example, benzotriazole (BTA) and its derivatives are restricted all over the world for the heavily toxic and environmentally hazardous materials. Therefore, it's time to find eco-friendly and non-toxic inhibitors to replace harmful ones[27, 28]. Ionic liquids (ILs) have been come up with for the purpose of preventing corrosion [29, 30], because ILs have quite a bit distinctly properties such as non-toxic, low vapour pressure, chemical stability and so on[31, 32], ILs have tendency to be perfect alternatives to replace traditional toxic corrosion inhibitors.

As a consequent, the purpose of this research is to estimate the corrosion-inhibition effect of 1-allyl-3-butylimidazolium bromine (Fig. 1) for X65 steel in 0.5 M H_2SO_4 aqueous solution. The inhibition properties of [ABIm]Br have been systematically studied using various effective methods, containing potentiodynamic polarization, EIS and SEM. Furthermore, quantum chemical calculations have been extensively employing to optimize [ABIm]Br structures and interpret the results of experiment. Last but not least, the adsorption properties of [ABIm]Br on X65 steel surface are investigate by molecular dynamics simulations. In conclusion, quantum chemical calculations and molecular dynamics simulations are further demonstrated experimental results in theory.

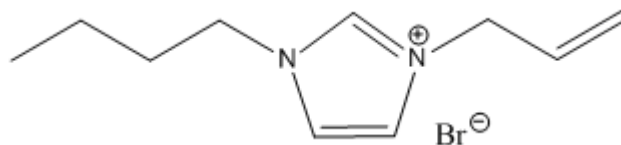


Figure 1. Molecular structure of 1-allyl-3-butylimidazolium bromine

2. EXPERIMENTAL

2.1. Materials and sample preparation

To fabricate the working electrode, the following chemical composition of X65 steel were used (wt.%): Si = 0.17%, Mn = 1.64%, Cr = 0.16%, Nb = 0.041%, C = 0.06%, Al = 0.035% and the

remainder Fe. In the experiment, 1-allyl-3-butylimidazolium bromine (99%), sulfuric acid (H_2SO_4 , AR) were used.

The X65 steel for electrochemical measurements were mechanically cut into $1.00\text{ cm} \times 1.00\text{ cm} \times 1.00\text{ cm}$ and the ones for weight loss tests were $2.00\text{ cm} \times 2.00\text{ cm} \times 1.00\text{ cm}$, while the specimens for surface analysis were $0.50\text{ cm} \times 0.50\text{ cm} \times 0.50\text{ cm}$. Meanwhile, electrochemical samples were embedded in epoxy leaving only side exposed to the test solution.

Before all experiments, the working surface was mechanically buffed with emery paper (from 400 to 2000 grit) up to a mirror-like bright surface, then syringed with distilled water, conducted through a so-called degreasing progress to remove smear in acetone and dried in hot air.

The composition of test solution was 0.5 M H_2SO_4 solution with adding various concentrations (1mM, 2.5mM, 5mM, 10mM) of 1-allyl-3-butylimidazolium bromine into base solution and the freshly prepared solution was employed at room temperature prior to each experiment. Except the theoretical calculations, all experiments were carried out in the air and a calibrated thermostat with a precision of 1 K was used to control the temperature of system.

2.2. Weight loss tests

The pretreated and weighted accurately X65 steel samples were immersed in test solutions which are 0.5 M H_2SO_4 in the absence and presence of various concentration of [ABIm]Br for 24 h at 298K, 1-10 mM of the investigated ILs was employed to explore the influence of [ABIm]Br concentration. Then, the coupons were washed thoroughly with H_2O and acetone, re-weighed. In order to reduce error, there are three parallel experiments during every condition and calculating the average value of corrosion rate[33].

2.3. Electrochemical tests

Electrochemical measurements including potentiodynamic polarization and EIS were carried out employing CHI660D electrochemical workstation with a typical three-electrode cell during various inhibitor concentrations in 0.5 M H_2SO_4 aqueous solution[34]. A saturated calomel electrode with the Luggin capillary (SCE) and a platinum electrode were served as reference electrode (RE) and counter electrode (CE) in the three electrode cell system, respectively. The working electrode had been mentioned above in detail. To be sufficient to obtain a nearly steady state (open circuit potential E_{ocp}), the working electrode was immersed in the test solution for 40 min prior to every experiment.

Subsequently, Potentiodynamic polarization curves were guaranteed by changing the potential (vs. SCE) automatically from -250 mV to 250 mV vs. OCP at a scan rate of 2 mV s^{-1} . The Tafel curves were analyzed by the way of extrapolation and corresponding data were obtained[35].

The EIS measurements were obtained in the scanned frequency range of 100 kHz-10 mHz using a small sinusoidal potential to perturb the system with amplitude of 5 mV at OCP. Besides, the AC impedance data were processed by employing the Zsimpwin 3.10 software. For each experimental

condition, the same experiment was usually performed to ensure the reliability and reproducibility of the experimental data.

2.4 Morphology analysis

The test X65 steel specimens were prepared as described. The surface morphologies of each X65 steel specimen after immersed in 0.5 M H₂SO₄ solution with and without 10 mM inhibitor at 298 K for 6 h in air atmosphere were characterized by scanning electron microscope (SEM). The samples were drastically washed and dried in the air to ensure that there are no residues still appending on the metal surface. The SEM images of the samples were analyzed at an accelerating voltage of 10 or 15 kV.

2.5 Computational details

Quantum chemical calculations toward anti-corrosion molecule were calculated using Gaussian 03W program. Which significant parameters including E_{HOMO} (the energy of highest occupied molecular orbital), E_{LUMO} (the energy of lowest unoccupied molecular orbital), ΔE (energy gap) = $E_{LUMO} - E_{HOMO}$, μ (dipole moment) were acquired, respectively. The structure of the ILs molecule was geometrically optimized by density functional theory (DFT), which has been widely utilized to predict the molecule properties [16, 36].

The Material Studio 6.0 software with Network Virtual Terminal ensemble was bear to research the interaction between the Fe (110) surface and [ABIm]Br cation. Besides, the molecular dynamics simulation was performed at a common given temperature (298K) with a time step of 1.0 fs and simulation time of 1000 ps. In addition, the processing of simulations had been reported in quite a lot documents[26].

3. RESULTS AND DISCUSSION

3.1 Weight loss measurements

Table 1. Corrosion rates (ν) and inhibition efficiencies (η) for X65 steel in 0.5 M H₂SO₄ solution with different concentrations of [ABIm]Br for 24 h at 298 K.

C (mM)	ν (g m ⁻² h ⁻¹)	η (%)	θ
0	24.34	/	/
1	13.31	45.31	0.4531
2.5	8.82	63.76	0.6376
5	5.22	78.54	0.7854
10	2.56	89.47	0.8947

Weight loss measurements are employed to further monitor the corrosion inhibition efficiency because it is quietly simple and reliable [37]. The inhibition results of the [ABIm]Br in the test solution for 24h at 298 K are obtained in Table 1. The rate of corrosion ($v \text{ g m}^{-2} \text{ h}^{-1}$), inhibition efficiency (η) and surface coverage (θ) are figured up as follows:

Error! Reference source not found. (1)

Error! Reference source not found. (2)

Error! Reference source not found. (3)

Here, S is the superficial area of samples in total, t is the immersion time (h), W_0 and W are the weight of samples without and with different inhibitor concentration, v_0 and v are the corresponding corrosion rates, respectively.

It is clearly seen that the rate of corrosion is decreased and inhibition efficiency is increased with the adding of [ABIm]Br compared to the blank. These results may attribute to the fact that there are more corrosion inhibitor molecules adsorbed on the X65 steel surface and surface coverage (θ) augments with the increase of [ABIm]Br [26, 37, 42]. The inhibition efficiency is up to 89.47% when the concentration of [ABIm]Br is 10mM. The inhibition efficiency of 1-allyl-3-butylimidazolium bromine ([ABIm]Br) is higher than 1-vinyl-3-ethylimidazolium bromide ([VEIM]Br) which has been researched by our group member in the same condition[43].

3.2. Potentiodynamic polarization curves

Potentiodynamic polarization measures for X65 steel are carried out and the media solutions are 0.5 M H_2SO_4 aqueous solution in the absence and various concentration of the ionic liquid inhibitor at 298 K. Typical potentiodynamic polarization curves are displayed in Fig. 2. The significant corrosion parameters are obtained by the linear extrapolation of the Tafel curves and listed in Table 2[44], containing corrosion potential (E_{corr}), corrosion current density (I_{corr}), Tafel constants (anodic and cathodic Tafel slopes, β_a and β_c , respectively) and inhibition efficiency (η) which can be calculated using the following formula:

Error! Reference source not found. (4)

Where **Error! Reference source not found.** stands for corrosion current densities without inhibitor in test solution, while **Error! Reference source not found.** is converse.

Table 2. The Potentiodynamic polarization parameters for the corrosion of X65 steel specimens in 0.5 M H_2SO_4 containing different concentrations of [ABIm]Br.

C(mM)	E_{corr} (mV)	$i_{corr}(\text{mAcm}^{-2})$	$\beta_a(\text{mVdec}^{-1})$	$\beta_c(\text{mVdec}^{-1})$	$\eta\%$
0	-455	1.964	154.4	124.4	/
1	-460	1.128	158.4	118.5	42.57
2.5	-468	0.5907	157.6	103.1	69.92
5	-469	0.3903	147.3	99.3	80.13
10	-467	0.1889	149.9	83.9	90.38

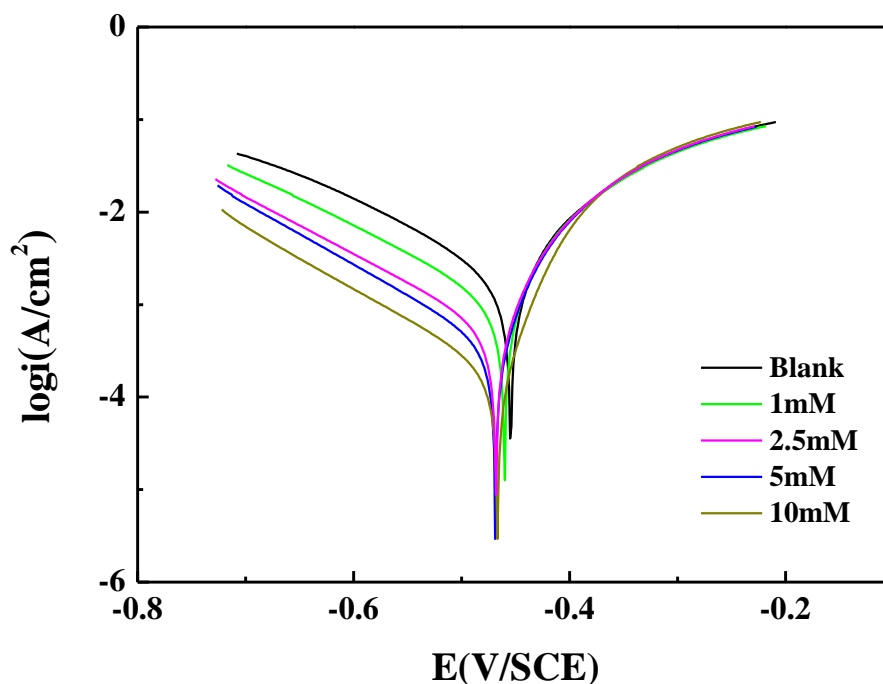


Figure 2. Potentiodynamic polarization curves for X65 steel coupons in 0.5 M H₂SO₄ in the absence and presence of [ABIm]Br.

The cathodic polarization curves show that I_{corr} has shifted to lower current densities with the addition of inhibitor, while there is no remarkable change in anodic current density even the adding of [ABIm]Br up to 10 mM. The rate of corrosion is directly proportional to the corrosion current density [45]. Which demonstrates that [ABIm]Br mainly inhibits the hydrogen ions reaction on the X65 steel surface to form H₂ in 0.5M H₂SO₄ medium, which bubbles from the metal surface[17], hence it acts as a proper cathodic inhibitor. Meanwhile we can see that the values of β_a and β_c are not changed dramatically with the addition of inhibitor concentrations, indicating that the inhibitors affect reactions on the electrode without changing the corrosion mechanism [46, 47]. Therefore, it may be inferred that [ABIm]Br is an effective inhibitor to X65 steel and the inhibition effect enlarges with the increase of [ABIm]Br concentration.

Inspection of the Fig. 2, cathodic polarization curves in the absence and presence of organic compound are incline to parallel, which suggests that the inhibitor of [ABIm]Br doesn't modify the mechanism of cathodic hydrogen evolution reduction in this process [2, 38-39]. Moreover, anti-corrosive efficiencies for X65 steel are obtained in Table 2. From the table, it clearly reveals that anti-corrosive efficiency increases in the addition of [ABIm]Br compared with the blank solution. It is distinctly observed that there is no largest change of E_{corr} (much less than 85mV) in the presence of [ABIm]Br, which indicates that the organic compound is considered as a mixed-type inhibitors and its cathodic action is predominant[37, 39-40, 42, 46], which means the inhibitors are mainly retards the cathodic hydrogen evolution reactions[40, 46]. Meanwhile, according to the documents[3,48] that

organic inhibitors are mixed type inhibitors in general by the simple blocking effect on the anodic and cathodic sites.

It is distinctly seen that I_{corr} drop sharply and η grow apparently with the increase of [ABIm]Br concentration, respectively. The highest inhibition efficiency was reached 90.38% when the adding of inhibitor is up to 10 mM. These results suggest that the organic molecules are effective to retard the corrosion of X65 steel, which may be due to the formation of protective film on the metal surface [49].

3.3. Electrochemical impedance spectroscopy (EIS)

Table 3. AC Impedance parameters acquired from the corrosion of X65 steel in 0.5 M H₂SO₄ solution including different concentrations of [ABIm]Br.

C (mM)	R_s ($\Omega \text{ cm}^2$)	CPE		R_{ct} ($\Omega \text{ cm}^2$)	L ($\Omega \text{ cm}^2$)	R_L ($\Omega \text{ cm}^2$)	$\eta(\%)$
		$Y_0(\times 10^{-6})$ $Ss^n \text{ cm}^{-2}$	n				
0	1.465	482.4	0.95	9.52	37.58	80.43	/
1	1.507	159.4	0.91	18.61	76.96	91.72	48.84
2.5	1.678	154.5	0.86	39.12	217.80	225.60	75.66
5	1.796	176.4	0.83	49.83	177.50	309.40	80.90
10	1.421	168.5	0.82	85.19	494.10	666.20	88.82

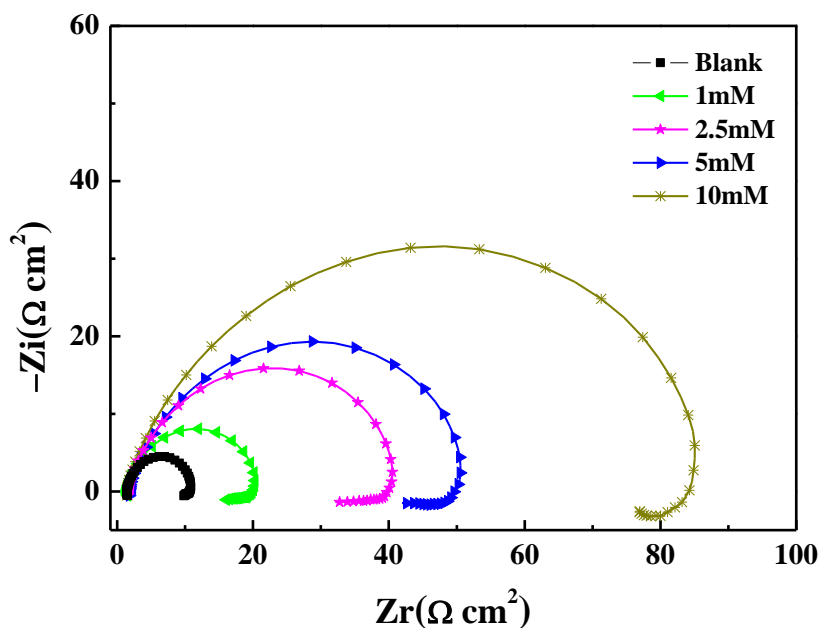


Figure 3. Nyquist plot for X65 steel samples in 0.5 M H₂SO₄ without and with various concentrations of [ABIm]Br.

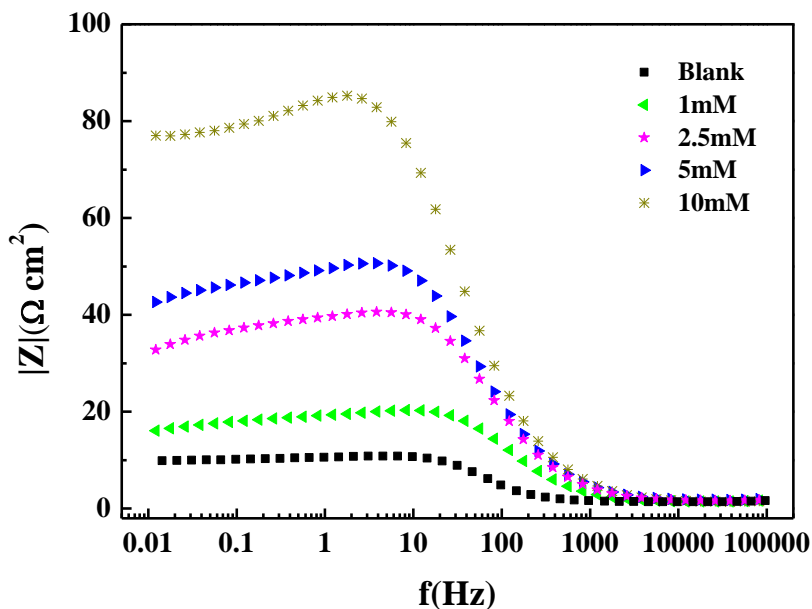


Figure 4. Bode modulus plot for X65 steel in 0.5 M H₂SO₄ in the absence and presence of [ABIm]Br.

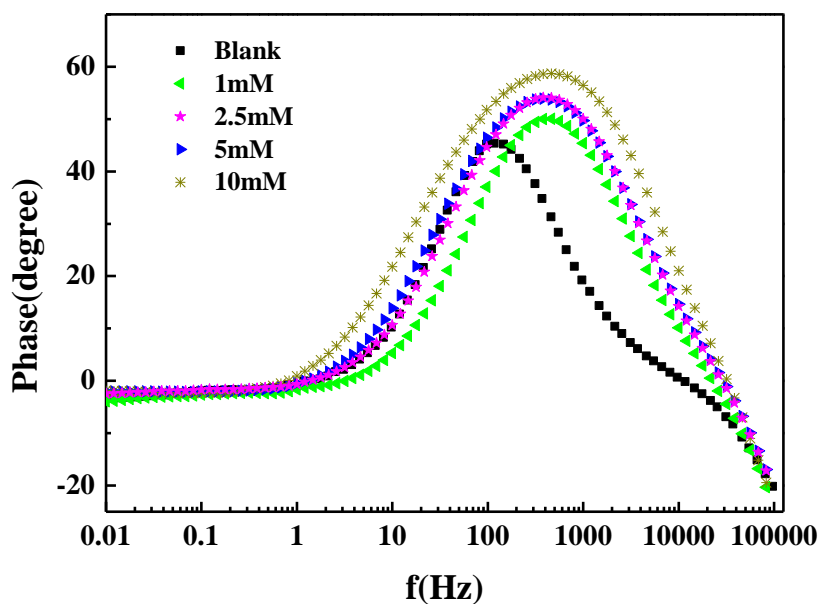


Figure 5. Bode phase angle plots for X65 steel in 0.5 M H₂SO₄ in the absence and presence of [ABIm]Br.

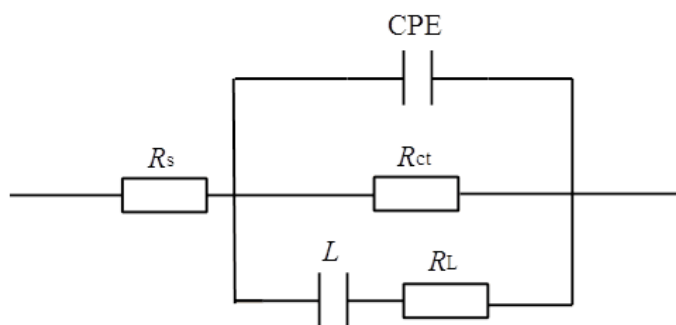


Figure 6. Equivalent circuit model used to fit the result of EIS tests.

The EIS technique has been widely applied into investigating corrosion behavior and mechanism for the advantage of accurately acquiring information on the processes of corrosion inhibition [41, 49-50]. In this paper, EIS technique is also employed to analyze the corrosion behavior of X65 steel in base solution (0.5 M H₂SO₄) without and with various concentrations of [ABIm]Br.

From the plots, we can distinctly observe that there is quite a few change of impedance response of X65 steel in test solution with the increase of inhibitor molecules[46]. The depressed sem-circle at high frequency domain generally related to the process of charge transfer and double layer behavior[2], arising from frequency dispersion in the result of the unflatness and inhomogeneity of the X65steel electrode surface, indicates that the reaction between electrode surface and test solution is primarily controlled by the process of charge transfer [38, 42]. Meanwhile, the dimension of the capacitive loop distinctly augments with the increase of [ABIm]Br, declaring [ABIm]Br adsorbed on the metal surface[13], while other changes almost don't occur, suggesting inhibitor molecule leaves hardly any influence on the corrosion mechanism[38, 51], while almost same results are obtained in Fig. 2. While the inductive loop at low frequency region ascribes to the adsorption of film resistance due to adsorption of a certain matter, such as intermediates、inhibitors and other accumulated products[1]. As seen from Fig. 4, there is a single CPE in the steel/solution interface, and the increase of $|Z|$ at low frequencies (in the left part of the figure) suggests a higher protection with the addition of [ABIm]Br, which may be correlated to the adsorption of inhibitor on the steel surface[14,52]. Also, only one time constant at the different concentrations of [ABIm]Br is observed in Bode-phase angle plots Fig. 5.

According to the above mentioned, proper equivalent circuit model fitted the result of EIS tests to model the steel / solution interface is designed in Fig. 6. The impedance parameters, including solution resistance (R_s), double-layer capacitance (C_{dl}), charge transfer resistance (R_{ct}), inductive elements of L and R_L , constant phase element (CPE, consisted of double layer capacitance C_{dl} and coefficient n) are listed in Table 3. The impedance of the constant phase element for a circuit is expressed as following equation [14]:

$$Z_{CPE} = \frac{1}{Y(j\omega)^n} \quad (5)$$

where Y is the coefficient of CPE, j is the imaginary root ($j^2 = -1$), ω is the angular frequency ($\omega = 2\pi f$) and n is the deviation parameter depended on the morphology of surface. It is easy to gain the information about the extent of non-idealization in capacitive behavior from the equation (5). According to the values of n , it is likely to distinguish between the behavior of an ideal capacitor ($n = 1$) and of other CPE (CPE can represent resistance ($n = 0$), inductance ($n = -1$) and Warburg impedance ($n = 0.5$))[38, 53]. The values of inhibition efficiency (η) can be calculated:

$$\eta = \frac{R_{ct} - R_{ct}^0}{R_{ct}} \times 100 \quad (6)$$

Where R_{ct}^0 and R_{ct} represent the charge transfer resistances in the absence and with various concentration of inhibitor, respectively.

From table 3, it is clearly that the values of R_{ct} increase as the same as cathode polarization curves, which may be caused by the protective layer, decreasing the electron transfer at the X65 steel/medium interface with the addition of the inhibitor.

So η is increased, which further proves that [ABIm]Br regards as a contributing corrosion inhibitor for X65 steel in 0.5 M H₂SO₄ medium. Conversely, the values of C_{dl} , which is described as the equations (7), have tendency to decrease as a whole with the addition of inhibitor[2, 26, 54].

$$C_{dl} = \frac{A\epsilon\epsilon_0}{d} \tag{7}$$

Where d is the thickness of electrical double layer, A is the effective surface area of X65 steel electrode, ϵ is the dielectric constant of solution and ϵ_0 is the vacuum permittivity. This model suggests that the decrease of C_{dl} may be caused by the decrease of ϵ and/or an increase in the thickness of the protective layer (d) which may stem from water molecules replaced gradual increasingly by [ABIm]Br molecules and the inhibitors effective adsorb at the electrode surface, which availably reduces the extent of the corrosion of metals[55]. The results of EIS measurements are in good agreement with the analysis of weight loss measurements and potentiodynamic polarization curves.

3.4. Adsorption behavior

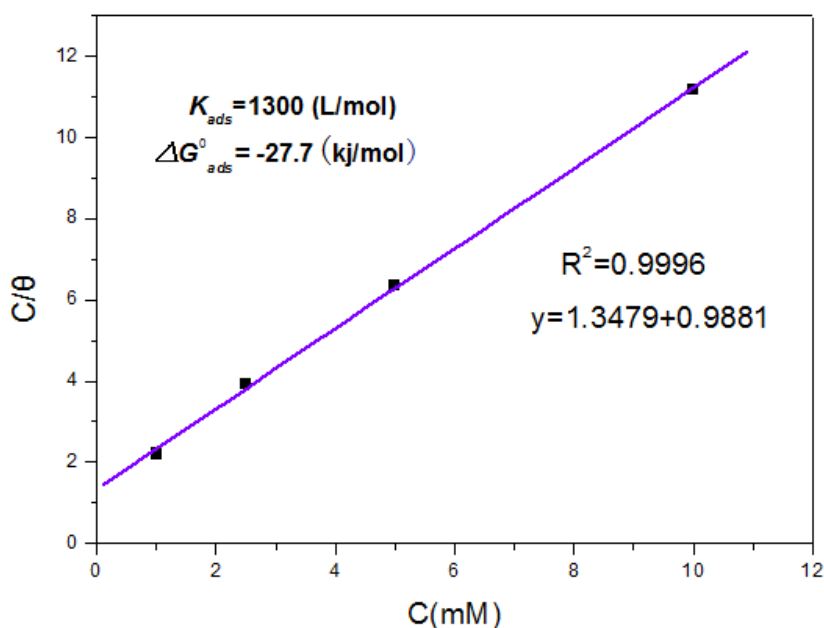


Figure 7. The relationship between C/θ and C and corresponding thermodynamic parameters for X65 steel in 0.5 M H₂SO₄ including various [ABIm]Br.

According to the report of E. Sadeghi Meresht et al, it is usually supposed that the adsorption function of inhibitors on the steel surface is the crucial step in an inhibition mechanism[1, 56]. Therefore, the corrosion inhibitors form a tight protective film to inhibit the corrosion of the metals by means of adsorbing on X65 steel surface via displacing water molecules[42], while adsorption isotherm can employ to study the adsorption property at metal/solution interphase. Hence, the investigated inhibitor was measured using various adsorption isotherms to fit the weight loss measurements. Nevertheless, Langmuir adsorption isotherm is the best described the process of adsorption[57], which can be expressed as follows[2, 14]:

$$\frac{C_i}{\theta} = \frac{1}{K_{ads}} + C_i \quad (8)$$

Where, C_i is the concentration of organic compounds, K_{ads} represents the adsorptive equilibrium constant for the process of adsorption and the values of the degree of surface coverage (θ) for the various presence of [ABIm]Br in the 0.5 M H_2SO_4 solution have been given by the equation (3) from the average of inhibition efficiency (η) of weight loss experiments.

From the Fig. 7, this isotherm explicitly manifests that Langmuir adsorption isotherm is the best described to fit experimental results, with correlation coefficient ($R^2 = 0.999$) and slope near 1. Meanwhile, it is quietly convenient to obtain the value of $1/K_{ads}$ (K_{ads} stands for the adsorption forces between the steel surface and inhibitor molecules) by the intercept of the plot on the y-axis, which can be used to calculate the standard adsorption free energy (ΔG_{ads}^0) as follows[2],

$$\Delta G_{ads}^0 = -RT \ln(55.5 K_{ads}) \quad (9)$$

Here, R and T represent the universal gas constant ($R = 8.314 \text{ J}\cdot\text{mol}^{-1}\text{K}^{-1}$) and absolute temperature (K), respectively. The constant of 55.5 is the molar concentration of water (mol/L)[9] and the value of K_{ads} is 1300 L/mol and the value of ΔG_{ads}^0 is -27.7 kJ/mol.

Generally, there is electrostatic binding between the charged molecules and the charged metals, that is physical adsorption when the negative value of ΔG_{ads}^0 is up to -20 kJ/mol, meanwhile the ones is negative than -40 kJ/mol, which represents chemisorption, including charge sharing or transfer between the inhibitor molecules and the metal surface to form a coordinate type of bond[18, 21]. In this paper, the value of ΔG_{ads}^0 calculated is ranged between -20~-40 kJ/mol, indicating that the adsorption mechanism of 1-allyl-3-butylimidazolium bromine in 0.5 M H_2SO_4 solution on the X65 steel substrate is consistent with physisorption and chemisorption [1].

3.5 Surface morphology analysis

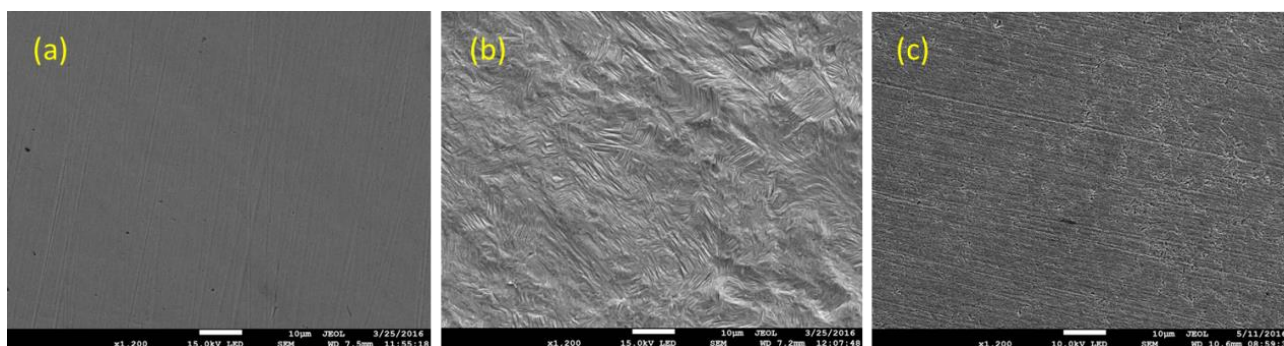


Figure 8. SEM images ($\times 1200$) of X65 steel specimens: without immersion in test solution (a); immersed in 0.5 M H_2SO_4 in the absence (b) and presence (c) of 10 mM [ABIm]Br.

The surface topography of X65 steel immersed in the 0.5 M H_2SO_4 aqueous solution without and with 10 mM [ABIm]Br are shown in Fig. 8. From SEM photographs, it is clearly seen that the surface of the prepared specimen is quietly smooth (a). The surface X65 steel was strongly damaged exposing in the aggressive solution, while the ones don't change obviously in the test solution with 10 mM inhibitor, suggesting that the adsorption of inhibitor molecules contributes to reduce the corrosion

rate. These results manifest the inhibitor molecules have effect on protecting metals by forming a compact film on the X65 steel surface and are in agreement with the electrochemical tests.

3.6 Quantum Chemical Calculation

Table 4. Corresponding quantum chemical parameters for the [ABIm]Br cation.

E_{HOMO} (eV)	E_{LUMO} (eV)	ΔE (eV)	μ (D)
-11.34	-5.0	6.34	3.5208

From above experimental analysis, we can know that the inhibitors decrease the rate of corrosion via forming a compact protective layer at metal/solution interface. Quantum chemical calculations[9, 20, 38, 58] have been extensively employed to further investigate the influence of molecular structure on the effect of corrosion inhibition, corresponding parameters, containing frontier molecular orbital energies (E_{HOMO} , E_{LUMO}), energy gap ($\Delta E = E_{LUMO} - E_{HOMO}$), dipole moment (μ) of the optimized geometrical structure ([ABIm]Br) closely associated with each other are listed in Table 4. Meanwhile, density functional theory (DFT) is used and pictures of HOMO and LUMO are shown in Fig. 9.

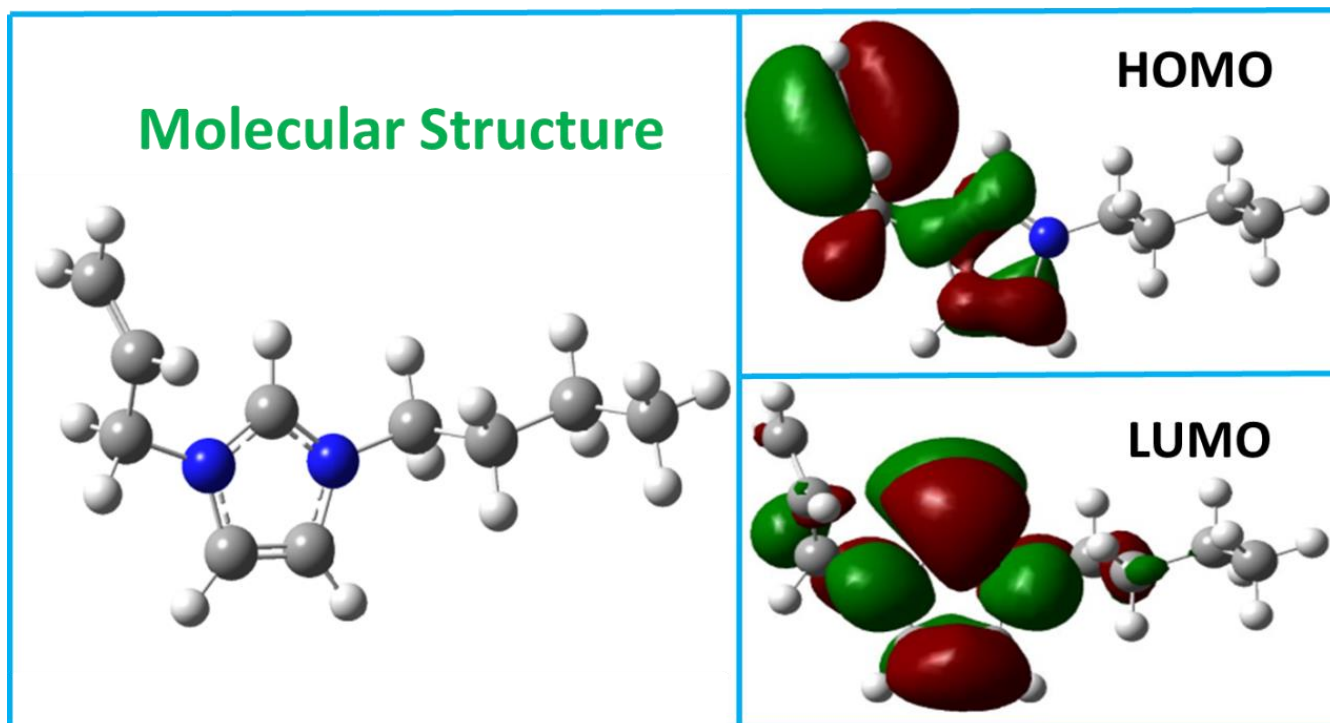


Figure 9. Molecular structure, HOMO and LUMO of [ABIm]Br cation.

It is well-known that there are in positive correlation between the value of E_{HOMO} and inhibition efficiency, namely, the inhibition efficiency enhances with the increase of E_{HOMO} , while a higher value

of E_{HOMO} shows the capability of the inhibitor to donate electrons to corresponding acceptors with a lower energy and vacant molecular orbitals. Conversely, the E_{LUMO} is reflected the ability of the organic compounds to gain electrons, while a lower value of E_{LUMO} suggests that the molecule would accumulate additional electrons from the metal surface. Therefore, the ΔE is in negative proportion to inhibition efficiency, since a lower value of ΔE indicates that the molecule is readily polarizable and easily accepted electrons from the metal[20, 59-60]. It is obviously seen that the electron density distribution of HOMO is almost lay in the imidazole ring and the ones for LUMO are mainly distributed imidazole ring and double bond in Fig. 9, which indicates that these are the active sites for adsorption of [ABIm]Br. In addition, we also should be pay attention to the value of μ , it was reported that a higher corrosion inhibition efficiency could obtain at a higher μ values according to the literature[36, 38, 61]. The high value of dipole moment is beneficial to adsorption owing to electrostatic interactions.

3.7. Molecular dynamic simulation

Molecular dynamic simulation (MD) has been employing to simulate the adsorption structure of inhibitor molecules on substrate surface. The equilibrium configuration of [ABIm]Br adsorbed on the Fe(110) surface is displayed in Fig.10.

From the side elevation drawing, we can see that the [ABIm]Br cation is almost flat-lying adsorbed on the Fe (110) surface via imidazole ring. The orientation of [ABIm]Br cation enlarges the degree of surface coverage, which could contribute to protect metal by minimizing the substrate surface area exposed in aggressive solution[16].

In addition, the energy of interaction between Fe (110) surface and organic compound computed via MD is 475.05 kJ/mol, which generally manifests that the adsorption is the primary mechanism of interaction between corrosion inhibitor and X65 steel[62], in other words, [ABIm]Br is a high-efficiency corrosion inhibitor to protect X65 steel in 0.5 M sulfuric acid solution, which is are in accordance with the above-mentioned.

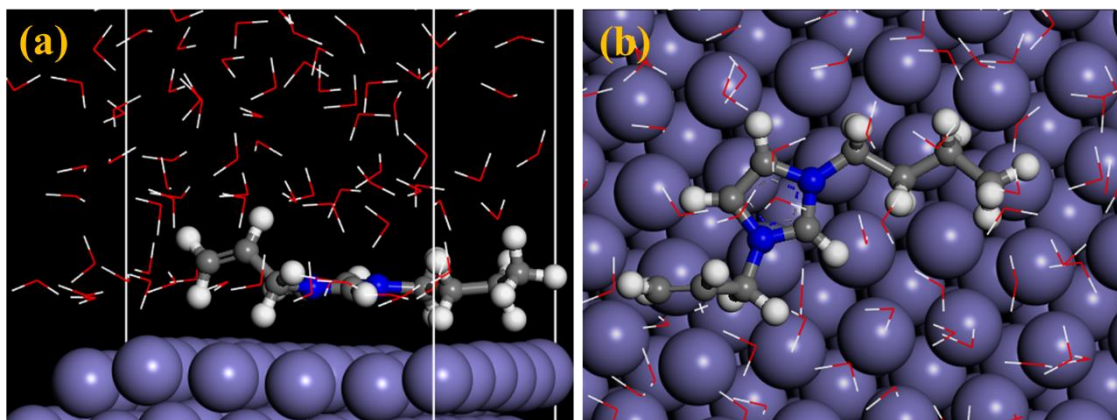


Figure 10. Equilibrium configuration for adsorption of [ABIm]Br on Cu (111) surface after optimization, (a) side view, (b) top view.

4. CONCLUSIONS

In this work, the inhibition efficiency of 1-allyl-3-butylimidazolium bromine on the X65 steel in 0.5 M H₂SO₄ solution was investigated by following characterization methods and the conclusions can be described as follows,

(1) [ABIm]Br was found to be an effective for X65 steel in 0.5 M H₂SO₄ aqueous solution by weight loss experiments and SEM. Besides, the effect of inhibition was mainly concentration dependent, that means the concentration of inhibitor have a significant influence on inhibition efficiency (η).

(2) Polarization measurements reveal that [ABIm]Br act as a mixed-type inhibitor mainly controlling the process of cathode corrosion.

(3) From the EIS data, we can know that charge transfer resistance (R_{ct}) increases dramatically with the adding of [ABIm]Br, suggesting that the inhibitor molecules are adsorbed on the X65 steel surface.

(4) It was found that the adsorption of the organic molecule on X65 steel substrate followed the Langmuir adsorption isotherm and the process of adsorption is an exothermic and spontaneous process.

(5) Results obtained from theoretical simulations show that the studied inhibitor is adsorbed powerfully on the X65 steel substrate by imidazole ring in a parallel.

ACKNOWLEDGMENTS

This research was supported by Natural Science Foundation of China (No. 21376282), Sail plan of Guangdong, China (No.2015YT02D025) and Project of Sichuan Provincial Department of Education (No.15ZB0297).

References

1. E. Sadeghi Meresht, T. Shahrabi Farahani, J. Neshati. *Corrosion Science*, 54 (2012) 36.
2. A. A. Farag, M. A. Hegazy. *Corrosion Science*, 74 (2013) 168.
3. J. Zhang, J. Wang, F. Zhu, M. Du. *Industrial & Engineering Chemistry Research*, 54 (2015) 5197.
4. A. Gajek, T. Zakroczymski, V. Romanchuk, P. Topilnytsky. *Chemical Technology*, 6 (2012).
5. G. E. Badr. *Corrosion Science*, 51 (2009) 2529.
6. I. Lozano, E. Mazario, C. O. Olivares-Xometl, N. V. Likhanova, P. Herrasti. *Materials Chemistry and Physics*, 147 (2014) 191.
7. H. Choi, Y. K. Song, K. Y. Kim, J. M. Park. *Surface and Coatings Technology*, 206 (2012) 2354.
8. M. A. Chidiebere, C. E. Ogukwe, K. L. Oguzie, C. N. Eneh, E. E. Oguzie. *Industrial & Engineering Chemistry Research*, 51 (2012) 668.
9. T. Sasikala, K. Parameswari, S. Chitra. *Oriental Journal of Chemistry*, 32 (2016) 1215.
10. M. Palomar-Pardavé, M. Romero-Romo, H. Herrera-Hernández, M. A. Abreu-Quijano, N. V. Likhanova, J. Uruchurtu, J. M. Juárez-García. *Corrosion Science*, 54 (2012) 231.
11. M. Behpour, S. M. Ghoreishi, M. Khayatkashani, N. Soltani. *Materials Chemistry and Physics*, 131 (2012) 621.
12. B. Gao, X. Zhang, Y. Sheng. *Materials Chemistry and Physics*, 108 (2008) 375.
13. M. Salah, Tawfik. *Journal of Molecular Liquids*, 216 (2016) 624.

14. M. A. Hegazy, M. Abdallah, M. K. Awad, M. Rezk. *Corrosion Science*, 81 (2014) 54.
15. M. A. Quraishi, A. Singh, V. K. Singh, D. K. Yadav, A. K. Singh. *Materials Chemistry and Physics*, 122 (2010) 114.
16. I. B. Obot, S. Kaya, C. Kaya, B. Tüzün. *Research on Chemical Intermediates*, 42 (2016), 4963.
17. M. M. Solomon, S. A. Umoren, I. I. Udosoro, A. P. Udoh. *Corrosion Science*, 52 (2010) 1317.
18. S. Zhang, Z. Tao, S. Liao, F. Wu. *Corrosion Science*, 52 (2010), 3126.
19. M. J. Bahrami, S. M. A. Hosseini, P. Pilvar. *Corrosion Science*, 52 (2010) 2793.
20. M. J. Bahrami, S. M. A. Hosseini, P. Pilvar. *Corrosion Science*, 52 (2010) 2793.
21. Y. Yang, G. Joshi, R. Akid. *Materials*, 8 (2015) 8728.
22. A. Joseph, Ronevich, P. Somerday, W. Chtics, San Marchi. *International Journal of Fatigue*, 82 (2016) 497.
23. M. Heydari, M. Javidi. *Corrosion Science*, 61 (2012) 148.
24. G. Gece. *Corrosion Science*, 53 (2011) 3873.
25. L. O. Olasunkanmi, I. B. Obot, M. M. Kabanda, E. E. Ebenso. *The Journal of Physical Chemistry C*, 119 (2015) 16004.
26. S. A. Umoren, I. B. Obot, Z. M. Gasem. *Ionics*, 21 (2014) 1171.
27. H. Wang, C. Yu, S. Huang. *Int. J. Electrochem. Sci.*, 10 (2015) 5827.
28. P. B. Matad, P. B. Mokshanatha, N. Hebbar, V. T. Venkatesha, H. C. Tandon. *Industrial & Engineering Chemistry Research*, 53 (2014) 8436.
29. A. Pourghasemi Hanza, R. Naderi, E. Kowsari, M. Sayebani. *Corrosion Science*, 107 (2016) 96.
30. L. C. Murulana, A. K. Singh, S. K. Shukla, M. M. Kabanda, E. E. Ebenso. *Industrial & Engineering Chemistry Research*, 51 (2012) 13282.
31. E. Kowsari, M. Payami, R. Amini, B. Ramezanzadeh, M. Javanbakht. *Applied Surface Science*, 289 (2014) 478.
32. H. Ashassi-Sorkhabi, M. Es'haghi. *Materials Chemistry and Physics*, 114 (2009) 267.
33. M. M. Solomon, S. A. Umoren, I. I. Udosoro, A. P. Udoh. *Corrosion Science*, 52 (2010) 1317.
34. L. Liu, Y. Zhang, X. Yin, J. Qian. *Surface and Interface Analysis*, 45 (2013) 949.
35. Y. Qiang, S. Zhang, S. Xu. *RSC Advances*, 5 (2015) 63866.
36. D. Daoud, T. Douadi, S. Issaadi, S. Chafaa. *Corrosion Science*, 79 (2014) 50.
37. I. B. Obot, N. O. Obi-Egbedi. *Corrosion Science*, 52 (2010) 198.
38. X. Zheng, S. Zhang, W. Li, L. Yin, J. He, J. Wu. *Corrosion Science*, 80 (2014) 383.
39. X. Li, S. Deng, H. Fu. *Corrosion Science*, 53 (2011) 302.
40. X. Wang, H. Yang, F. Wang. *Corrosion Science*, 53 (2011) 113.
41. H. Wang, C. Yu, S. Huang. *Int. J. Electrochem. Sci.*, 10 (2015) 5827.
42. A. A. Farag, M. R. Noor El-Din. *Corrosion Science*, 64 (2012) 174.
43. N. Chen, S. Zhang, Y. Qiang, S. Xu, X. Ren. *Int. J. Electrochem. Sci.*, 11 (2016) 7230.
44. D. Guzmán-Lucero, O. Olivares-Xometl, R. Martínez-Palou. *Industrial & Engineering Chemistry Research*, 50 (2011) 7129.
45. X. Wang, X. Tang, L. Wang. *Journal of Natural Gas Science and Engineering*, 21 (2014) 474.
46. M. A. Migahed, A. M. Al-Sabagh, E. A. Khamis, E. G. Zaki. *Journal of Molecular Liquids*, 212 (2015) 360.
47. Q. B. Zhang, Y. X. Hua. *Electrochimica Acta*, 54 (2009) 1881.
48. S. A. Abd El-Maksoud, *Int. J. Electrochem. Sci.*, 3 (2008) 529.
49. Sherif, M. El-Sayed. *Int. J. Electrochem. Sci.*, 8 (2013) 9360.
50. L. Y. Xu, M. Li, H. Y. Jing, Y. D. Han. *Int. J. Electrochem. Sci.*, 8 (2013) 2069.
51. X. Li, S. Deng, H. Fu. *Corrosion Science*, 53 (2011) 302.
52. M. A. Hegazy, A. M. Hasan, M. M. Emara, M. F. Bakr, A. H. Youssef. *Corrosion Science*, 65 (2012) 67.
53. K. Stanly. Jacob, Geetha Parameswaran. *Corrosion Science*, 52 (2010) 224.
54. S. Deng, X. Li. *Corrosion Science*, 55 (2012) 407.

55. Ahmed.Y. Musa, Ramzi T. T. Jalgham, Abu Bakar Mohamad. *Corrosion Science*, 56 (2012) 176.
56. A. Asan, M. Kabasakaloglu, M. Işıklan. *Corrosion Science*, 47 (2005) 1534.
57. M. A. Migahed, A. A. Farag, S. M. Elsaed, R. Kamal, M. Mostfa, H. Abd El-Bary. *Mater. Chem. Phys*, 125 (2011) 125.
58. Y. Qiang, S. Zhang, S. Xu. *Int. J. Electrochem. Sci*, 11 (2016) 3147.
59. L. Guo, S. Zhu, S. Zhang, Q. He, W. Li, *Corrosion Science*, 87 (2014) 366.
60. J. Fu, S. Li, Y. Wang, X. Liu, L. Lu. *Journal of Materials Science*, 46 (2011) 3550.
61. N. O. Obi-Egbedi, I. B. Obot, *Corrosion Science*, 53 (2011) 263.
62. I. B. Obot, N. O. Obi-Egbedi, E. E. Ebenso. *Research on Chemical Intermediates*, 39 (2013) 1927.

© 2016 The Authors. Published by ESG (www.electrochemsci.org). This article is an open access article distributed under the terms and conditions of the Creative Commons Attribution license (<http://creativecommons.org/licenses/by/4.0/>).